ISSN (Print) 1226-1750
ISSN (Online) 2233-6656
Journal of Magnetics 20(1), 40-46 (2015) http://dx.doi.org/10.4283/JMAG.2015.20.1.040

Accuracy Analysis of Magnetic Resonance Angiography and Computed Tomography Angiography Using a Flow Experimental Model

Yeong-Cheol Heo[1,2], Hae-Kag Lee[3], Cheol-Soo Park[4], and Jae-Hwan Cho[1]*

[1]*Department of International Radiological Science, Hallym University of Graduate Studies, Seoul 135-841, Korea*
[2]*Department of Radiology, Kyung Hee University Hospital at Gang-dong, Seoul 134-727, Korea*
[3]*Department of Computer Engineering, Soonchunhyang University, Asan 336-745, Korea*
[4]*Department of Radiological Science, Hallym Polytechnic University, Chuncheon 200-711, Korea*

(Received 3 February 2015, Received in final form 12 February 2015, Accepted 12 February 2015)

This study investigated the accuracy of magnetic resonance angiography (MRA) and computed tomography angiography (CTA) in terms of reflecting the actual vascular length. Three-dimensional time of flight (3D TOF) MRA, 3D contrast-enhanced (CE) MRA, volume-rendering after CTA and maximum intensity projection were investigated using a flow model phantom with a diameter of 2.11 mm and area of 0.26 cm^2. 1.5 and 3.0 Tesla devices were used for 3D TOF MRA and 3D CE MRA. CTA was investigated using 16 and 64 channel CT scanners, and the images were transmitted and reconstructed by volume-rendering and maximum intensity projection, followed by conduit length measurement as described above. The smallest 3D TOF MRA measure was 2.51 ± 0.12 mm with a flow velocity of 40 cm/s using the 3.0 Tesla apparatus, and 2.57 ± 0.07 mm with a velocity of 71.5 cm/s using the 1.5 Tesla apparatus; both images were magnified from the actual measurement of 2.11 mm. The measurement with the 16 channel CT scanner was smaller (3.83 ± 0.37 mm) than the reconstructed image on maximum intensity projection. The images from CTA from examination apparatus and reconstruction technique were all larger than the actual measurement.

Keywords : magnetic resonance angiography, computed tomography angiography, flow phantom, vascular diameter

1. Introduction

Cerebrovascular diseases are classified into hemorrhagic and ischemic. While historically there has been a higher proportion of the hemorrhagic type, more recently the proportion of ischemic cerebrovascular disease has increased [1]. Internal and surgical treatments have been developed for the treatment of ischemic cerebrovascular disease; many studies have reported on intracranial stenting since the introduction of this non-surgical intervention. Lee *et al.* evaluated the influences of natural history, medication treatment, extracranial and intracranial bypass surgery, intracranial angioplasty, and intractranial stenting with the risk of stroke due to intracranial arteriostenosis and treatment indication; intracranial stenting carried a low risk and was effective in cases of relapse [2]. For intracranial stenting it is important to understand the degree of stenosis through various radiologic examinations and to decide of the stent size. In-stent restenosis or thrombosis from wall shear stress is possible when a stent is too large or too small [3]. Computed tomography (CT), magnetic resonance imaging (MRI) and conventional angiography are the typical examinations used to measure vessel cross-section prior to surgery and to discern the relationship between other vessels apart from the target vessel [4]. CT is the standard imaging examination for the cerebrovascular diseases as it can be done quickly, can diagnose both intracerebral and cerebral blood flow depending on the image reconstruction, has high sensitivity and is able to obtain the vessel information without overlap between the vessel and surrounding structures through three-dimensional (3D) imaging [5-7].

Magnetic resonance angiography (MRA) includes time of flight (TOF) MRA and contrast enhanced (CE) MRA. There is no radiation exposure with increased imaging quality for both approaches, whose use is gradually increasing as a differential examination for non-invasive cerebrovascular assessment [8]. Attributes of 3D TOF and

*Corresponding author: Tel: +82-70-8680-5900
Fax: +82-2-3453-6618, e-mail: 8452404@hanmail.net

3D CE MRA include very high degrees of sensitivity, specificity, positive prediction, and negative prediction for vascular stenosis [9].

Clinical stroke guideline published in 2009 recommended MRA and CTA as essential examinations for treatment planning, such as stent size, as they provide an accurate understanding of the pathophysiology of cerebrovascular diseases [4]. The ability of each approach to reflect the actual measurement is necessary to determine, given the differences in vessel imaging. The present study used a vessel phantom that recognized the actual lumen to determine the accuracy of the imaged size compared to the actual measurement.

2. Materials and Methods

2.1. Phantom model

A conduit made out of polyethylene resin (diameter of 211 mm and area of 0. 26 cm^2) was penetrated through the body of the phantom and connected to both ends to allow inflow and outflow. The phantom was round with a length of 19 cm, height of 5 cm, and diameter of 5 cm. The polyethylene resin was minimally affected by X-ray and radio frequency. The interior of the phantom contained water as a human tissue equivalent matter. The inflow section of phantom was designed to connect the contrast media auto injector to allow the quantitative inflow of the fluid.

2.2. Study Methods

A 3.0 Tesla MR System (Achieva Release 2.5; Philips, Holland) and 1.5 Tesla MR System (Achieva Release 1.5; Philips, Holland) were used for 3D TOF MRA and 3D CE MRA. An eight-channel sensitivity encoding (SENSE) HEAD coil was used for the 3.0 Tesla system and examined with 3D fast field echo (FFE) sequence technique with the following parameters: field of view (FOV) $180 \times 180 \times 12$ mm^3, matrix 400×215, TR/TE 20/3.5 ms, total slice 25, flip angle 20°, phase encoding direction R-L, NEX 1, chunk 1, slice thickness 0.5 mm, slice orientation transverse, and total scan time 21.9 sec. The same coil and 3D FFE sequence was used for the 1.5 Tesla system with the following parameters: FOV 180 mm^2, matrix (F × P) 400×128, TR/TE 13/2.3 ms, total slice 25, flip angle 20°, phase encoding direction right-left, NEX 1, chunk 1, slice thickness 0.5 mm, slice orientation transverse, and total scan time 14.3 sec. The fluid was inserted through a non-pulsed contrast media auto injector with flow velocities of 0.4, 0.7, 1.1, 1.4, 1.8, 2.1, 2.5, 2.8, 3.2, or 3.5 ml/sec. The flow velocity was calculated as quantity of flow ÷ conduit area. The conduit area was 0.26 cm^2 and the actual flow velocity was 11.4 cm/sec with the insertion of 0.4 ml/sec. The actual conduit flow velocity calculated from the equation is presented in Table 1. 3D TOF images examined using 1.5 and 3.0 Telsa were reconstructed to maximum intensity projection (MIP) using an advanced tool provided with the device. The reconstructed histogram used the reset value provided with the equipment to minimize variables of image measures. Distance measurement provided by the advanced tool was used for the 30 measurements taken at the center of the coronal plane (Fig. 1). 3D CE MRA was done using a 16 channel SENSE Neuro-Vascular coil on a 3.0 Tesla MR System using the 3DT1FFE Sequence technique using the following parameters: FOV: $350 \times 350 \times 80$ mm^3, matrix (F × P): 716×715, TR/TE: 5.4/2.0 ms, total slice: 160, flip angle: 20°, phase encoding direction: R-L, NEX: 1, slice thickness: 0.5 mm, slice orientation: coronal, CE profile: CENTRA, keyhole: no, and total scan time: 61 sec. An 8 channel SENSE Neuro-Vascular coil was used for the 1.5 Tesla MR System with the 3DT1FFE Sequence technique using the following parameters: FOV: 350 mm^2, matrix (F × P): 515×257, TR/TE: 4.9/1.7 ms, total slice: 150, flip angle: 40°, phase encoding direction: R-L, NEX: 1, slice thickness: 0.5 mm, slice orientation: coronal, CE profile: CENTRA, keyhole: no, and total scan time: 14.3 sec. The fluid for 3D CE MRA was prepared with Gd-DTPA 2.5 ml diluted into 1000 ml of saline solution. The total volume of 150 ml diluted fluid was inserted through the automated injector at 2 ml/sec. 3D TOF images examined on the 1.5 and 3.0 Telsa were reconstructed to MIP as described above. The procedures for the reconstructed histogram and distance measurement are also described above (Fig. 2). CTA was examined using a Brilliance 64 channel CT scanner (Philips, Holland) and a Brilliance 16 channel CT scanner (Philips, Holland). The settings for the 64 channel CT scanner were kVp: 120, mAs: 200,

Table 1. The Flow Velocity in the tube.

Pressure (ml/sec)	0.4	0.7	1.1	1.4	1.8	2.1	2.5	2.8	3.2	3.5
Flow Velocity (cm/sec)	11.4	20	31.4	40	51.5	60	71.5	80.1	91.5	100.1

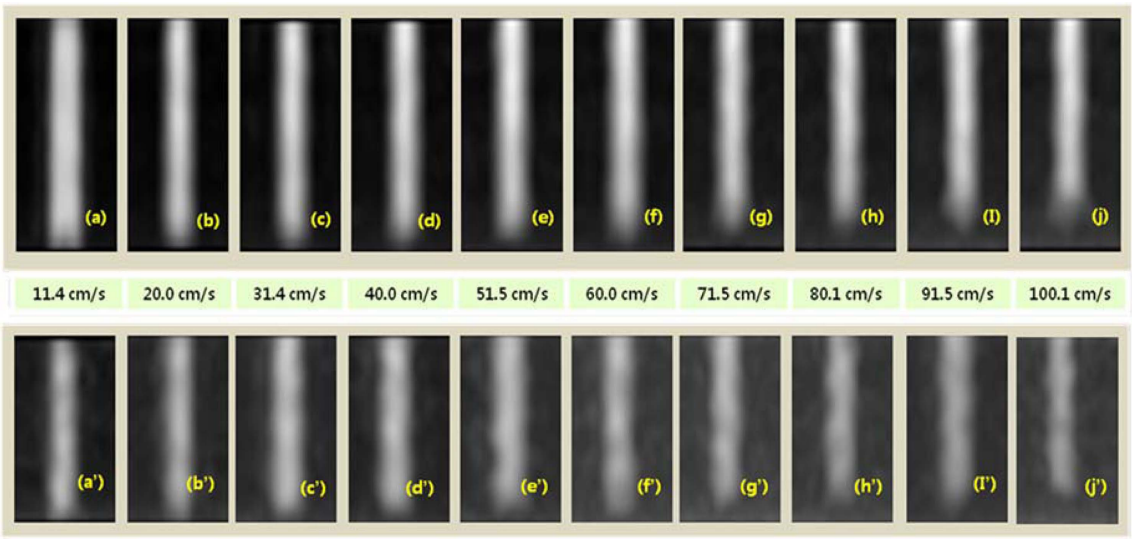

Fig. 1. (Color online) 3D time of flight images from 1.5 and 3.0 Tesla according to flow velocity. Panels A-J depict 3.0 Tesla 3D time of flight images and panels A'-J' depict 1.5 Tesla 3D time of flight images.

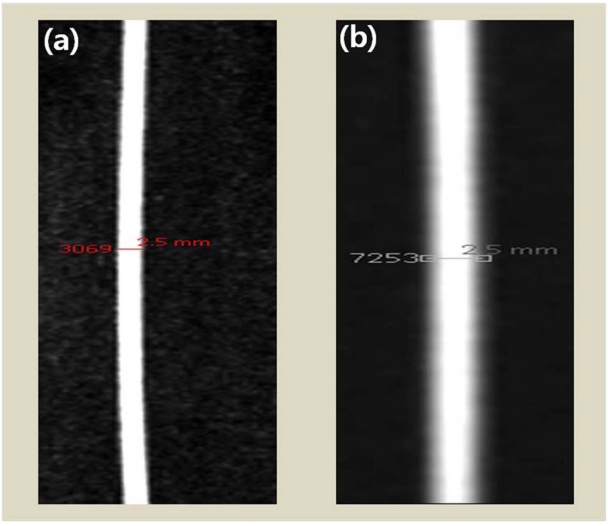

Fig. 2. (Color online) Contrast enhanced magnetic resonance angiography images at 3.0 Tesla (a) and 1.5 Tesla (b).

FOV: 200, pitch: 0.671, thickness/gab: 0.8/0.4 mm, matrix: 512 × 512, slice: 257, collimation: 64 × 0.625 (4 cm), and rotation time: 0.5 sec. The settings for the 16 channel CT scanner were kVp: 120, mAs: 200, FOV: 200, pitch: 0.688, thickness/gab: 0.8/0.4 mm, matrix: 512 × 512, slice: 257, collimation: 16 × 0.75 (1.2 cm), and rotation time: 0.5 sec. Non-ionic iodine contrast media (IODIXANOL; 21 ml containing 270 mg iodine) was inserted at 3 ml/sec through the contrast media auto injector. The examined image was transmitted to an Aquarius intuition edition ver 4.4.6.85.2800 3D specific work station (Terarecon, USA), then reconstructed using volume rendering and MIP (Fig. 3). For the 3D image reconstruction technique, a 3D volume browser histogram reset value was applied to volume rendering, and a 3D neuro1 histogram reset value was applied to MIP. The reset value for both imaging techniques was ramp-up window width: 201, window level: 244, opacity: 1.00, and right-recline triangle window width: 126, window level: 192, opacity: 0.40. Distance

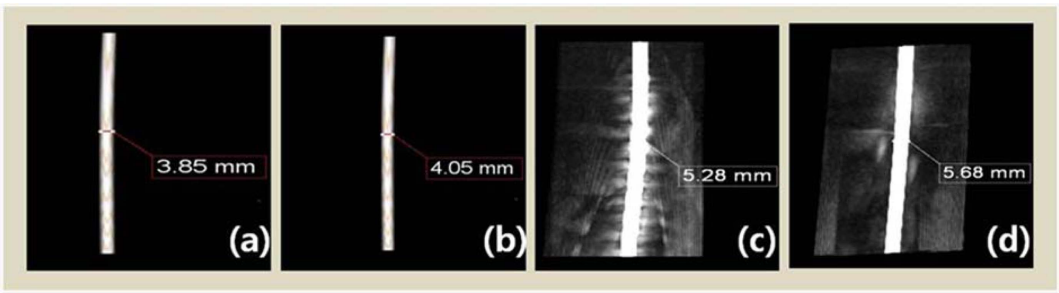

Fig. 3. (Color online) Measure the length of (a) 16 Channel volume rendering, (b) 64 Channel volume rendering, (c) 16 Channel maximum intensity projection, (d) 64 Channel maximum intensity projection.

measurement was determined from the work station by 30 measurements at the center of the coronal plane.

Statistical analyses were done using SPSS (version 18.0, USA, Chicago) for Windows. ANOVA was done on the mean length according to the flow velocity for the analysis of 1.5 and 3.0 Tesla 3D TOF. For more accurate difference determination, post-hoc analysis was conducted using Tukey B[a]. The correlation of flow velocity, measured length, and measured length in the different devices were analyzed with Pearson Correlation coefficient. One sample t-test on the actual measure of 2.11 mm and the measured value that was closest to the actual measurement. CTA NOVA was conducted on the mean value of reconstructed images from the 16 and 64 channel CT scanners, and post-hoc analysis. The one sample t-test was conducted on the actual measure of 2.11 mm and the measured value that was closest to the actual measurement.

3. Results

3.1. Measurement of lumen length in terms of flow velocity of 3D TOF MRA

From the measurement of lumen length in terms of flow velocity within the conduit, the smallest measure was 2.51 ± 0.12 mm with a velocity of 40.0 cm/sec, and the largest measure was 2.65 ± 0.89 mm with a velocity of 91.5 cm/sec on 3.0 Tesla. For 1.5 Tesla, the smallest measure was 2.57 ± 0.07 mm with a velocity of 71.5 cm/sec, and the largest measure was 2.63 ± 0.07 mm with the velocity of 91.5 cm/sec ($p < 0.05$). For 3.0 Tesla, the value measured at 40 cm/sec, which was the closest value to the actual measurement, was 0.40333 mm larger than the actual measure. For 1.5 Tesla, the value measured at 71.5 cm/sec was 0.4667 mm larger than the actual measure ($p < 0.05$) (Table 2). From the correlation analysis between the flow velocity and length measurement, the difference in length measured on the devices and the increase in flow velocity did not correlate, and there was a 0.181 positive correlation due to the different device ($p < 0.05$) (Table 3).

Table 2. Measurement of lumen length in terms of flow velocity of 3D time of flight magnetic resonance angiography.

Velocity (cm/sec)	3.0Tesla Mean (mm)	1.5Tesla Mean (mm)	P
11.4	2.62±0.08	2.58±0.10	0.00
20	2.61±0.06	2.61±0.86	
31.4	2.62±0.09	2.61±0.08	
40	2.51±0.12	2.58±0.09	
51.5	2.56±0.09	2.60±0.08	
60	2.58±0.09	2.58±0.06	
71.5	2.55±0.07	2.57±0.07	
80.1	2.61±0.06	2.61±0.06	
91.5	2.65±0.89	2.63±0.07	
100.1	2.63±0.10	2.61±0.07	
Equipment	(Mean - 2.11) mm		P
3.0Tesla (velocity : 40 cm/s)	0.40		0.00
1.5Tesla (Velocity : 71.5 cm/s)	0.46		0.00

3.2. Measurement of lumen length of 3D CE MRA

From 3D CE MRA there was no mean difference between 3.0 Tesla and 1.5 Tesla as the values were 2.61 ± 0.06 mm and 2.65 ± 0.156 mm, respectively ($p > 0.05$). 3D CE MRA conducted using 3.0 Tesla examination produced a value 0.50000 mm larger than the actual value. The value from 1.5 Tesla examination was 0.54333 mm larger than the actual value ($p < 0.05$) (Table 4).

3.3. Measurement of lumen length of CTA

For lumen length with image reconstruction, the volume

Table 4. Measurement of lumen length of 3D contrast enhanced magnetic resonance angiography.

	3.0Tesla	1.5Tesla	P
Mean (mm)	2.61±0.06	2.65±0.16	0.16
Equipment	(Mean - 2.11) mm		P
3.0Tesla 3D CE MRA	0.50		0.00
1.5Tesla 3D CE MRA	0.54		0.00

Table 3. Correlation analysis of flow velocity and measured length using 1.5 and 3.0 Tesla.

		3.0Tesla	1.5Tesla	Flow Velocity
3.0Tesla	Pearson correlation coefficient	1	0.18	0.08
	P	-	0.00	0.20
1.5Tesla	Pearson correlation coefficient	0.18	1	0.72
	P	0.00	-	0.21
Flow Velocity	Pearson correlation coefficient	0.75	0.72	1.00
	P	0.20	0.21	-

Table 5. Measurement of lumen length of computed tomography angiography.

Reconstruction	64Channel	16Channel	P
	Mean (mm)	Mean (mm)	
3D Volume Rendering	4.01±0.16	3.83±0.37	0.00
3D Maximum Intensity Projection (MIP)	5.46±0.19	5.34±0.63	
Equipment	(Mean - 2.11) mm		P
64Channel Volume Rendering	1.91		0.00
16Channel Volume Rendering	1.67		0.00

rendering technique value of 4.01 ± 0.16 mm was smaller than the 5.46 ± 0.19 mm MIP value using the 64 channel CT scanner. The same trend was observed using the 16 channel CT scanner; the volume rendering value of 3.83 ± 0.37 mm was smaller than the MIP value of 5.34 ± 0.63 mm ($p < 0.05$). When the image measured using the 64 channel for CTA was reconstructed with the volume rendering technique, the measured value was 1.90633 mm larger than the actual value. On 16 channel, the measurement was 1.66767 mm larger than the actual value ($p < 0.05$) (Table 5).

4. Discussion

TOF MRA and CE MRA are the most representative examinations for CTA. TOF MRA is non-invasive and is free of contrast media complications since it does not use contrast medium, instead obtaining images using blood flow. TOF MRA provides information on vessel conformation and functional information, and allows high definition images of blood vessels within a relatively short time. These attributes have spurred its popularity [10-13]. TOF MRA produces a low signal by saturating the signal from a stationary object, and uses blood flow to yield a contrast difference between stationary anatomical objects and blood vessels [13]. Therefore, in TOF MRA variables related to imaging technique and fluid property may affect the images. The current study aimed to determine the actual reflection of the image according to the flow velocity and the changes in terms of examination devices through the change in the flow velocity of TOF MRA. There was no difference in the measured length in terms of the flow velocity, and there was a 0.181 positive correlation between 3.0 Tesla and 1.5 Tesla. The images were augmented by 0.40333 and 0.46667 mm in 3.0 Tesla and 1.5 Tesla, respectively. Choi *et al.* [14]. reported that signal-to-noise ratio and contrast-to-noise ratio were increased when flow velocity was reduced, and opined that the signal intensity of a fluid proportionally increases to the flow velocity until it reaches critical velocity. In this study, we measured the difference between the measured length and the flow velocity, which was different from the investigation of the difference between signaling and flow velocity. The difference in measured length may occur from the different signals. Hence, the present results and those of Choi *et al.* [14]. significantly correlated. There was no difference in the measured length according to the flow velocity, indicating that the change in signal intensity would not affect the measured lengths in MIP. This is because MIP is a technique that only produces an image of the maximum value above the critical values of the whole image. Therefore, stationary components become saturated and represent the low signal, with flow being the high signal. The low signal becomes obscured due to a phase difference arising from the flow velocity. The difference between the stationary and flow matter is bigger than the difference of signal loss from the phase difference [15]. The difference in measured length from different devices is probably due to the variables related to the imaging techniques, which include repetition time, echo time, flip angle, slice thickness, and the matrix [13]. In this study there were difference in the repetition time, echo time, and matrix between the two Tesla techniques due to the difference in the default signal-to-noise ratio and difference in relaxation time according to the magnetic field strength. Use of a computer simulation model showed that the probability of restenosis within a stent is high when the size of the stent is large or small, so that it is better to use the stent that is the same size as the blood vessel.3 In this study, both 1.5 and 3.0 Tesla had magnified images regardless of the change in the flow velocity. In MIP, depth information is lost as 3D information is projected with the maximum value onto a 2D plane, and during the post process the images often are magnified due to matrix change [16-18]. In this study, the images obtained with TOF MRA were reconstructed using MIP, which was why the images were magnified relative to the actual measurement. In terms of the measured length between 3.0 Tesla and 1.5 Tesla, the measures were almost the same, and both devices resulted in the images

that were magnified from the actual measurement. The image resolution in 3D CE MRA was dependent on the how the fundamental K-space is filled (i.e., sequential view ordering, conventional centric view ordering, elliptical centric view ordering). The filling methods differ according to how the center of the K-space is filled, which is responsible of the contrast. Sequential view ordering fills more than 60% of the K-space and appears to have the highest signal strength and contrast ratio. But, because it is hard to catch the moment of conversion from artery to vein image, imaging the artery is difficult. On the other hand, elliptical centric view ordering fills more than 40% of the K-space, making it easy to image the artery. However, the signal strength and contrast ratio is less than those of sequential view ordering. Conventional centric view ordering fills 50% of the K-space; its advantages and disadvantages somewhat in between sequential view ordering and elliptical centric view ordering [19].

The centric technique used in the study employed elliptical centric view ordering in both the 1.5 and 3.0 Tesla modes, and had the lowest signal strength and contrast ratio. However, elliptical centric view ordering is used to generate an image with least venous phase included. The parameters of signal strength and contrast ratio in 3D CE MRA were similar for 1.5 and 3.0 Tesla modes. Also, images were routinely magnified relative to the actual measure due to the error that occurred from the MIP image reconstruction (which also occurred for 3D TOF MRA).

CTA is a non-invasive, accurate approach that features a very short examination time. The introduction of multi detector CT has increased the sensitivity and specificity of the approach [20, 21]. However, presently CTA images were magnified relative to the actual measure using both the MIP and volume rendering techniques, and featured the most magnified image when compared to other devices. In CT, artifacts occur due to severe calcification lesion or concentrated contrast media, and blooming artifact (the examined object is larger than the actual size) has been reported. In this study, concentrated contrast media was used as the fluid. So, blooming artifact was very likely the source of the magnified images. Also the difference in magnification of measured length may have occurred due to the post treatment process. A study that used a phantom to measure the diameter of volume rendering technique and MIP reported volume rendering to be more accurate in 2-4 mm stenosis [22], which was also evident in the present study. Generally, volume rendering changes the degree of transparency and allows spontaneous visualization of the inside and the surface, and can make the image totally transparent or opaque according to the reconstructive object. Inaccuracy in the description of the boundary is not suitable for the accurate measurement. However, the opaque volume rendering has the almost same effect as the surface rendering image, which allows the significant boundary images to be obtained. In this study the concentrated contrast media was used to produce the surface volume rendering effect in the volume rendering technique; it produced less magnified images than MIP.

The blood vessel phantom used in this study could not reflect the characteristics of the actual vessels, and the fluid used in each examination was different to actual blood. Also, the flow of the fluid could not simulate the pulsating model. These differences were the limitations in this study. The difference in flow velocity resistance occurred due to the difference in conduit used in the phantoms, and signal differences also occurred in viscosity and magnification resonance images as the fluid was used instead of actual blood, Especially, in the T1 value, the image signal strength proportionally increases in a linear fashion as the concentration of matter increases, hence the MR signal will change according to blood flow. Secondly, the viscosity of fluid used in each examination was different. Saline solution, GA-DTPA diluted in saline solution, and concentrated non-ionic iodine contrast media were used according to the characteristics of each examination. Hence, the images from each examination were different. Thirdly, we could not simulate pulsating blood flow. Therefore when this study is applied in a clinical practice, those differences should be considered.

5. Conclusion

3D TOF MRA and 3D CE MRA used for CTA produce values that are augmented relative to the actual measurement. The present results provide evidence that the blood vessel model phantom will assist in the understanding of the principals of the various imaging techniques for blood vessels, such as MRA and CTA, and will provide fundamental data for the future design of experimental models.

Acknowledgments

Yeong-Cheol Heo and Hae-Kag Lee equally contributed to this work. They are co-first authors. This work was supported in part by the Soonchunhyang University Research Fund.

References

[1] H. J. Lee, O. K. Park, J. C. Gang, Y. K. Shin, S. L. Lee,

and M. J. Jing, J. Korean Med. Assoc. **34**, 758 (1991).
[2] Lee, B. H. Neurointervention **2**, 30 (2007).
[3] H. Y. Chen, J. Hermiller, A. K. Sinha, M. Sturek, L. Zhu, and G. S. Kassab, J. Appl. Physiol. **106**, 1686 (2009).
[4] D. H. Seo, H. S. Gang, D. W. Kim, S. K. Park, Y. Song, S. H. Shin, S. H. Yu, S. O. Kwon, J. H. Na, H. J. Bae, C. W. Oh, K. H. Yu, B. H. Yun, B. C. Lee, J. H. Heo, G. S. Hong, S. C. Hong, and I. S. Park, Kor. J. Cerebrovascular Surgery **13**, 279 (2011).
[5] H. J. Jeon, H. J. Lee, K. M. Kim, Y. S. Kim, Y. Ko, and S. J. Oh, J. Korean Neurosurg. Soc. **33**, 345 (2003).
[6] M. Matsumoto, M. Sato, M. Nakano, Y. Endo, Y. Watanabe, and T. Sasaki, J. Neurosurg. **94**, 718 (2001).
[7] K. K. Kim, C. H. Choi, S. W. Lee, S. W. Cha, and K. S. Song, Kor. J. Cerebrovascular Surgery. **7**, 12 (2005).
[8] J. H. Lee, T. S. Jung, K. Y. Lee, and S. H. Seo, J. Korean Soc. Magn. Reson. Med. **15**, 234 (2011).
[9] M. Cirillo, F. Scomazzoni, L. Cirillo, M. Cadioli, F. Simionato, A. Iadanza, M. Kirchin, and C. Righi, Anzalone N. Eur. J. Radiol. **82**, 853 (2013).
[10] P. J. Nederkoorn, Y. van der Graaf, B. C. Eikelboom, A. van der Lugt, L. W. Bartels, and W. P. Mali, AJNR Am. J. Neuroradiol. **23**, 1779 (2002).
[11] S. Beslic, Radiol. Oncol. **38**, 5 (2004).
[12] C. Lévy, J. P. Laissy, V. Raveau, P. Amarenco, V. Servois, M. G. Bousser, and J. M. Tubiana, Radiology **190**, 97 (1994).
[13] Y. Korogi, M. Takahashi, N. Mabuchi, H. Miki, S. Fujiwara, Y. Horikawa, T. Nakagawa, T. O'Uchi, T. Watabe, and H. Shiga, Radiology **193**, 181 (1994).
[14] C. G. Choi, M. H. Han, J. H. Park, and K. H. Jang, J. Korean Soc. Radiol. **36**, 729 (1997).
[15] S. H. Shin and D. S. Hwang, JKSMRM **16**, 67 (2012).
[16] C. Jackowski, E. Aghayev, M. Sonnenschein, R. Dirnhofer, and M. J. Thali, International Journal of Legal Medicine **120**, 165 (2006).
[17] E. K. Fishman, D. R. Ney, D. G. Heath, F. M. Corl, K. M. Horton, and P. T. Johnson, Radiographics **26**, 905 (2006).
[18] J. Lee, T. S. Chung, K. Y. Lee, and S. H. Suh, J. Korean Soc. Magn. Reson. Med. **15**, 234 (2011).
[19] Y. G. Kim, MRI in Practice, Academia, Seoul, 2013.
[20] H. S. Yong, J. Korean Med. Assoc. **50**, 25 (2007).
[21] U. J. Schoepf and P. Costello, Radiology **230**, 329 (2004).
[22] K. A. Addis, K. D. Hopper, T. A. Iyriboz, Y. Liu, S. W. Wise, C. J. Kasales, J. S. Blebea, and D. T. Mauger, AJR Am. J. Roentgenol. **177**, 1171 (2001).